A Roll-Aware Vehicle Stability Control Algorithm for Heavy Commercial Road Vehicles

Shravan S. Devadiga[1], Indra Mandal[2], Pavel Vijay Gaurkar[3], Mahesh Shridhare[4], Sriram Sivaram [5], and Shankar C. Subramanian[6]

***Abstract*— Vehicle stability control systems enhance maneuvering safety by intervening when the driver cannot maintain yaw stability or mitigate rollover risk. Additionally, by strategically interacting with the foundational Antilock Brake System, a safe braking response is ensured when demanded during cornering. This study presents a physics-motivated, logic-driven, roll-aware stability controller employing a tanh-based switching function to correct yaw instability and monitor rollover severity through differential braking. The proposed controller is evaluated in a Hardware-in-the-Loop (HiL) framework against a baseline Direct Yaw Moment Control formulation. Results indicate a 54% reduction in speed drop during high-speed cornering due to smoother yaw correction. Although a marginal reduction in yaw-rate tracking was observed under combined cornering and braking, it was accompanied by reduced control chattering, lower peak sideslip, and improved stopping distance, demonstrating a favourable performance trade-off. Both controllers prevented rollover in the Fishhook maneuver; however, the proposed strategy achieved a 75% reduction in total wheel lift-off time, outperforming the baseline formulation.**

***Keywords*—Differential Braking, Electronic Stability Control, Roll-Yaw Control, Untripped Rollover Prevention.**

I. Introduction

According to the latest data from the Ministry of Road Transport and Highways (MoRTH), India recorded 480,853 road accidents in 2023, out of which 33% were fatal [1]. Heavy Commercial Road Vehicles (HCRVs), such as trucks and buses, were involved in 10.9% of the total accidents. Many of these road accidents may occur when the driver misjudges the steering input or braking needed to safely navigate through obstacles and corners. This lack of judgement can lead to loss of directional stability of the vehicle, and consequently poor lane-keeping performance or rollover [2]. In these scenarios, active vehicle safety systems such as Electronic Stability Control (ESC) can potentially reduce vehicle instabilities and road accident fatalities. The ESC system stabilises the vehicle through differential braking so as to generate a corrective yaw moment without steering intervention, and is directly compatible with pneumatic brake hardware in HCRVs [3].

Advanced model-based ESC methods can provide strong performance by capturing the yaw and roll dynamics through the model and accordingly preserve directional and roll stability as presented in [4]. However, the need for tyre parameters, difficult-to-measure states (e.g., sideslip), and substantial computation, complicates deployment on production-intent brake ECUs [5]–[7]. The ESC algorithm presented in [8] was designed to work with readily available sensor data and an underlying ABS, however it was not developed considering excessive roll. The coupling between yaw and roll behaviour was discussed in [9], where conditions corresponding to decoupled and coupled roll-yaw instability were identified. Additionally, [10] demonstrated that while yaw stability control improves yaw dynamics and indirectly benefits roll, it does not fully mitigate rollover risk unless a dedicated roll controller is added. Although commercial ESC systems are widely available and deployed in the market [11], [12], the underlying control methodologies and design frameworks remain largely proprietary and are not disclosed in the public domain.

This study fills in these gaps and proposes a logic-based, roll-aware ESC algorithm capable of ensuring directional and roll stability of the vehicle. To ensure the tractability of the ESC algorithm across various maneuvers including emergency braking during cornering, it needs to be integrated with a foundational ABS algorithm.

A. Overview of ESC-ABS Architecture

A schematic representation of the proposed ESC architecture is shown in Fig. 1. Electronic Stability Control (ESC) functions as a supervisory layer that ensures vehicle stability through differential braking by coordinating lower-level brake controllers such as ABS. The ABS actuator controller regulates brake chamber pressure while compensating for pneumatic delays [13]. Based on the measured yaw rate, reference yaw rate, and load transfer ratio (LTR), the stability control unit computes the corrective action required to preserve yaw stability and mitigate rollover. Two operating modes are defined: ESC-only and ESC+ABS. The ESC Mode Selection block determines whether stability correction is realised via direct brake pressure modulation or through

*The authors thank the Madras Engineering Industries Private Limited, Chennai, India, for their support of this research through the grant RB21221488EDMADA008265. The authors also acknowledge the funding provided by the Ministry of Skill Development and Entrepreneurship, Government of India, through the grant EDD/14-15/023/MOLE/NILE.

[1]Research Scholar, Department of Engineering Design, Indian Institute of Technology Madras, Chennai, India. ed22d402@smail.iitm.ac.in

[2]Research Scholar, Department of Engineering Design, Indian Institute of Technology Madras, Chennai, India. ed24s014@smail.iitm.ac.in

[3]Lead Engineer, Controls Division, Madras Engineering Industries Private Ltd., Chennai, India. pavelgaurkar@gmail.com

[4]Madras Engineering Industries Private Ltd., Chennai, India. shridhare@mei.co.in

[5]Madras Engineering Industries Private Ltd., Chennai, India. ssivaram@mei.co.in

[6]Professor, Department of Engineering Design, Indian Institute of Technology Madras, Chennai, India. shankarram@iitm.ac.in

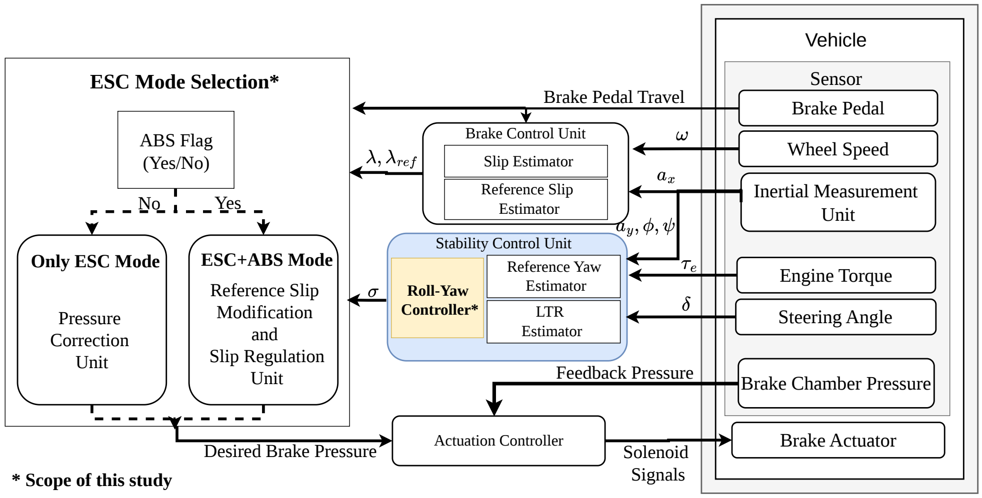

Fig. 1: ESC–ABS architecture

slip regulation. In cornering-only conditions, the controller directly generates a yaw or roll correction, which is translated into differential brake pressure commands. When braking induces significant slip, and ABS intervention is required, the controller switches to a reference slip modification mode [8]. In this mode, stability correction is achieved by modifying the reference slip. The reference slip, estimated from wheel slip [14], [15], gauges the attainable tyre–road force and is regulated according to [16], with stability corrections embedded through slip adaptation. Therefore, the vehicle stability controller determines corrective action for yaw and roll stability based on yaw rate tracking error and LTR, and realises this correction either via direct differential braking or through reference slip modification when ABS is active.

B. Vehicle Stability Control

A typical Stability Control Unit comprises a Yaw stability controller and a reference yaw rate generator. As presented in [10], a dedicated roll controller would be beneficial to fully mitigate rollover threat in addition to yaw stability control. The scope of this study is restricted to the hybrid controller development, hence an existing yaw reference generator inspired by [17] is utilised for controller evaluation and benchmarking. To evaluate the impact of integrating a dedicated roll correction, an existing direct yaw control algorithm is chosen as a benchmark.

The yaw-rate control based ESC presented in [8] adopts a sliding variable constructed from the yaw-rate error and uses a Power-Rate-Exponential-Reaching-Law (PRERL)-inspired mapping to generate a correction term. The controller requires the normalized yaw-rate tracking error,

$$s[k] = \frac{r[k] - r_{\text{ref}}[k]}{\max\big(|r_{\text{ref}}[k]|, \varepsilon_r\big)}, \tag{1}$$

where $\varepsilon_r > 0$ avoids division by very small $|r_{\text{ref}}[k]|$. The error is mapped to the scalar correction magnitude as

$$\chi[k] = K_0 \, \frac{|s[k]|^{\frac{1}{2}}}{0.5 + 0.5\,\exp\big(-|s[k]|\big)}, \tag{2}$$

where $K_0 > 0$ is a tuning gain.

The correction term is mapped to a modification in the reference slip to be used for wheel slip regulation in an underlying ABS algorithm, since this was designed to work with only combined cornering and braking maneuver. Although this formulation indirectly mitigates roll by limiting yaw, it does not explicitly capture roll dynamics. Additionally, it does not provide the methodology for correcting yaw instability during cornering-only maneuvers when ABS is untriggered.

To achieve a deployable control strategy applicable to both cornering-only and combined cornering–braking maneuvers, while simultaneously addressing rollover mitigation, a roll-aware rule-based stability controller is developed and benchmarked against the aforementioned formulation. The scope of the control algorithm implementation is restricted to fully laden single-unit twin-axle trucks operating on a homogenous wet asphalt road ($\mu = 0.5$). The roll stability was evaluated using untripped rollover threatened manuevers on a dry asphalt road ($\mu = 0.8$).

II. Methodology

A logic-based yaw-roll controller design would ideally require the yaw error–yaw correction map to have zero bias, linear sensitivity at low errors to emulate the tire-model low-slip region, and minimal controller chattering. Additionally, to circumvent excessive speed reduction during cornering-only maneuvers, saturation at large errors to avoid excessive correction and a deadzone to avoid intervention at small errors are desirable. Other nonlinear mappings can satisfy subsets of these requirements, however, the hyperbolic tangent was selected due to its zero bias, near-linear behaviour around the origin, smooth bounded saturation, and ease of slope tuning through a single gain parameter. Hence, a tanh-based sigmoid function with a deadzone, as depicted in Fig. 2, was adopted for the stability control unit, in contrast to the exponential sigmoid function presented in Eq. (2).

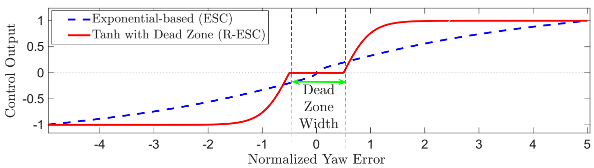

Fig. 2: Sigmoid functions for combined roll-yaw control.

A. Yaw-rate supervision

The normalised yaw-rate tracking error is formulated as:

$$s_y[k] \triangleq \frac{r[k] - r_{\text{ref}}[k]}{\max(|r_{\text{ref}}[k]|\,,\ r_\epsilon)}, \tag{3}$$

where $r_\epsilon > 0$ is a normalisation floor.

The dead zone in the tanh function helps in smoothening the switching. It is defined as:

$$\zeta_y[k] \triangleq \max(0,\ |s_y[k]| - s_{\text{dead}})\,, \tag{4}$$

where $s_{\text{dead}} > 0$ is the dead-zone width. This finally provides the bounded yaw severity as

$$\sigma_{\text{y}}[k] \triangleq \tanh(k_y \zeta_y[k])\,, \tag{5}$$

where $k_y > 0$ is the slope parameter.

The detection of understeering and oversteering tendencies is essential for determining the appropriate differential braking action required to generate the corrective yaw moment. To this end, the turn-direction, $d_t[k] = \text{sign}(r_{\text{ref}}[k])$, is subsequently employed to classify the vehicle's lateral stability state. The understeer-oversteer flag is computed as $\mathbb{I} = \text{sign}(d_t[k]\, s_y[k])$, where $\mathbb{I} = 1$ or -1 indicates oversteer tendency or understeer tendency respectively.

The above DYC algorithm is combined with an LTR-based formulation to further ensure roll stability, in addition to yaw correction for vehicle trajectory maintenance.

B. Rollover supervision: Hyperbolic-tangent severity map

In addition to the measured yaw rate $r[k]$ and the reference yaw rate $r_{\text{ref}}[k]$ for yaw correction, the proposed hybrid yaw-roll controller requires the estimated LTR, which is widely used as a rollover-risk indicator [18]. The LTR thresholds for rollover prevention are pre-defined for simplicity and are treated as tuning parameters. A binary rollover-prevention activation state $\mathbb{I}_{\text{r}}[k] \in \{0, 1\}$ is updated using the LTR thresholds LTR_{on} and LTR_{off}:

$$\mathbb{I}_{\text{r}}[k] = \begin{cases} 1, & \text{if } \mathbb{I}_{\text{r}}[k-1] = 0 \ \&\ \text{LTR} \geq \text{LTR}_{\text{on}}, \\ 0, & \text{if } \mathbb{I}_{\text{r}}[k-1] = 1 \ \&\ \text{LTR} \leq \text{LTR}_{\text{off}}, \\ \mathbb{I}_{\text{r}}[k-1], & \text{otherwise.} \end{cases} \tag{6}$$

Equation ((6)) enforces hysteresis directly in the update equation, reducing switching in the presence of measurement fluctuations. When rollover prevention is active, a bounded continuous rollover severity, $\sigma_{\text{r}}[k] \in [0, 1]$, is computed using a tanh map:

$$\sigma_{\text{r}}[k] = \mathbb{I}_{\text{r}}[k] \frac{(\tanh(k_r\, (\text{LTR[k]} - l_m)) + 1)}{2}, \tag{7}$$

where $l_m = \frac{LTR_{on} + LTR_{off}}{2}$, and k_r is the slope parameter.

C. Rollover-prioritised yaw attenuation

To ensure rollover mitigation dominates when rollover risk is elevated, the yaw severity is attenuated as a function of rollover severity:

$$a_y[k] = (1 - \kappa)\sigma_{\text{r}}[k], \tag{8}$$

where a_{y} is the yaw correction attenuation factor, and $\kappa \in [0, 1]$ sets the attenuation strength. Thereby the effective yaw severity is modified as:

$$\sigma_{\text{y,eff}}[k] \triangleq \sigma_{\text{y}}[k]\, a_y[k]. \tag{9}$$

Both the roll and the yaw correction terms are provided as outputs from the Stability Control Unit and are further processed by the ESC Mode Selection block to ensure the driver's brake demand is taken into consideration.

D. ESC Mode Selection and Dual-Mode Operation

The overall vehicle stability needs to be ensured irrespective of the driver's intervention by braking. There can be scenarios where the driver demands mild braking or demands maximum braking in the middle of a cornering maneuver. Additionally, the driver may not intervene with the required yaw correction. These scenarios need to be accounted for to ensure delivery of a robust vehicle stability unit. Hence, a dual-mode philosophy is adopted by overlaying the non-braking pressure for yaw or roll correction, with braking-phase reference slip modification to ensure optimal braking when needed in addition to stable cornering.

1) Non-Braking Mode (Differential Pressure Overlay): During non-ABS-intervened braking, the detection of vehicle instability triggers a corrective brake-pressure overlay which aims to generate a compensatory yaw moment. The corrective pressure is linearly mapped to the yaw and roll correction factor, and is further applied to the inner wheels or outer wheels based on the understeer or oversteer tendency. The trade-off here is minimizing vehicle speed reduction as the driver requires vehicle navigation with minimal braking.

Rollover-prevention braking: A symmetric and front-biased brake distribution vector is chosen for simplicity and is shaped by the rollover risk factor σ_r, which translates to the following scalar rollover-prevention pressure command:

$$\mathbf{p}_{b,r}[k] \triangleq P_{\text{r,max}} \sigma_r[k] \mathbf{g}_r, \tag{10}$$

where $\mathbf{g}_r$ is the pressure distribution vector.

Yaw stabilisation braking: Similarly the yaw-control pressure command is computed as,

$$\mathbf{p}_{b,y}[k] \triangleq P_{\text{y,max}}\ \sigma_{\text{y,eff}}[k] \mathbf{g}_y, \tag{11}$$

where $P_{y,max}$ is the maximum yaw-control pressure, and $\mathbf{g_y}$ denotes the pressure distribution gain vector which switches between inner wheel or outer wheel braking based on understeer-oversteer flags. The net corrective pressure per wheel, $\mathbf{p}_{b,\text{overlay}}[k]$ is determined as a sum of the yaw and roll corrective pressures:

$$\mathbf{p}_{b,\text{overlay}}[k] \triangleq \mathbf{p}_{b,y}[k] + \mathbf{p}_{b,r}[k]. \tag{12}$$

If the driver has demanded mild braking then the corrective brake pressures are simply added to the driver demanded brake pressures, however the final desired pressure is selected between the maximum of the driver demand and the controller demand. This is to ensure the level of conservative navigation rests at the driver's demand. The required brake pressure is defined as,

$$\mathbf{p_{b,ij}}^{\text{req}}[k] = \max\big(\mathbf{p}_{b,\text{drv}}[k], \mathbf{p}_{b,\text{drv}}[k] + \mathbf{p}_{b,\text{overlay},ij}[k]\big), \tag{13}$$

where $\mathbf{p}_{b,\text{drv}}[k]$ is the driver-requested pressure.

2) Braking Mode (Reference Slip Modification): During a combined cornering and braking maneuver, where the driver applies full braking and likely triggers ABS intervention, the ESC algorithm adopts a methodology where the objective is maintaining vehicle stability and avoiding wheel lock with the end goal of stopping the vehicle at the earliest. This is accomplished by correcting the desired pressure of the ABS to account for the directional or roll stability correction. The desired pressure of the ABS algorithm is determined by the wheel slip tracking error with respect to a reference slip. The reference slip at each wheel is modified by the ESC algorithm to account for the required yaw or roll correction. Let $\boldsymbol{\lambda}_0[k]$ be the nominal reference slip vector provided by the brake controller unit as depicted in Fig. 1. The desired slip vector is initialised as $\boldsymbol{\lambda}_{\text{desired}}[k] \triangleq \boldsymbol{\lambda}_0[k]$. When the ABS flag is active, yaw stabilization is implemented through reference slip modification rather than yaw pressure overlay, ensuring compatibility with the brake controller. The reference slip is modified by providing a bias based on the yaw correction factor. The bias is formulated as:

$$\Delta\lambda[k] \triangleq \min(\lambda_{\text{bias,max}}\sigma_{\text{y,eff}}[k],\ \lambda_{\text{bias,max}}), \tag{14}$$

where $\lambda_{\text{bias,max}} > 0$ is the maximum slip reduction permitted. Let the minimum reference slip be defined as $\lambda_{\text{min,safe}} > 0$ to ensure minimal non-zero braking.

The desired slip is modified as:

$$\lambda_{\text{des,ij}}[k] \triangleq \max(\lambda_{0,\text{ij}}[k] - \Delta\lambda[k],\ \lambda_{\text{min,safe}}). \tag{15}$$

As a design choice, based on understeer or oversteer tendency the reference slip of the front outer or rear inner wheel is modified. The desired slip is provided to the slip-regulation unit, which overrides the driver brake demand to ensure optimal braking while preserving vehicle stability.

III. Experimental Evaluation

This section delves into the evaluation of the proposed stability controller which is programmed in MATLAB Simulink®, and evaluated using a Hardware-in-Loop (HiL) setup equipped with pneumatic brake hardware and a high-fidelity vehicle dynamics simulation software.

A. Hardware-in-loop setup

This subsection presents the HiL setup, depicted in Fig. 3, used for ESC framework evaluation. The setup includes four Type-20 brake chambers, each equipped with an Electro-Pneumatic Regulator (EPR), which serves as a brake actuator and enables differential braking by metering out compressed air to the brake chamber from a reservoir, proportional to the voltage applied across the EPR. The reservoir is maintained at 8 bar pressure using a compressor. To enable feedback and pressure correction, each brake chamber is equipped with a pressure sensor. The input to the EPR and output from the pressure sensors are relayed by the IPG XPack4®, a real-time computer with 1.3 GHz clock speed, to the simulated vehicle running on IPG TruckMaker®, a high-fidelity vehicle dynamics simulation environment.

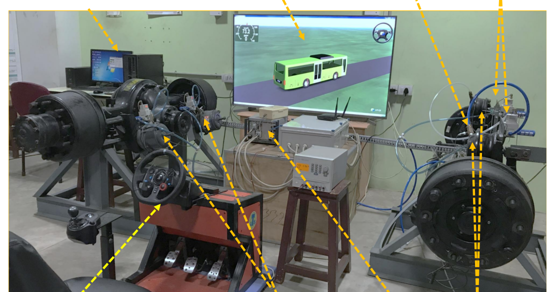

Fig. 3: HiL setup integrating IPG TruckMaker® and the pneumatic brake hardware of a 4×2 HCRV.

B. Evaluation Methodology and Results

This section discusses the evaluation of the proposed Stability Control algorithm integrated with an existing ABS algorithm. A fully laden vehicle (16200 kg) is subjected to a J-turn maneuver on a wet asphalt road ($\mu = 0.5$). In accordance with the ESC testing standards [3], the vehicle traversed an initial straight segment of 22.9 m at 48 km/h, followed by a $120°$ turn of radius 45.7 m, with constant steering input to ensure a steady-state cornering. Additional tests were conducted at an initial speed 65 km/h over a $180°$ turn of radius 100 m. Furthermore, a fish-hook maneuver, as specified in the same standard, was performed to evaluate roll stability control. The performance of the proposed Roll-aware ESC (R-ESC) algorithm is compared against the existing ESC algorithm and the Open Loop configuration with emphasis on improved stability while reducing excessive corrective braking and pneumatic actuation effort relative to conventional ESC. The impact of the intervention of the ESC and R-ESC algorithms towards the overall vehicle stability through differential braking is gauged through step-steer cornering tests, fishhook maneuver tests, and combined braking plus cornering tests, results of which are presented in Tab I. Additionally, air consumption towards braking was noted using a flowmeter to gauge the relative control effort.

TABLE I: Summary of ESC performance metrics corresponding to respective maneuvers.

Sr. No.	Maneuver	Initial speed (km/h)	Turn radius (m) and angle (deg)	Algorithm	Performance metrics					
					Braking distance (m)	Max sideslip angle (deg)	MATE Yaw-rate (rad/s)	Speed drop (m/s)	Mean roll angle (deg)	Mean LTR
1 2	Only cornering	48	45.7 m – 120°	ESC R-ESC	N/A N/A	2.34 **1.95**	**0.03** 0.04	6.36 **4.61**	NRT NRT	NRT NRT
3 4 5	Braking + cornering	48	45.7 m – 120°	ABS ESC R-ESC	40* 37 **37**	6.76 3.98 **3.86**	0.05 **0.03** 0.03	N/A N/A N/A	NRT NRT NRT	NRT NRT NRT
6 7	Only cornering	65	100 m – 180°	ESC R-ESC	N/A N/A	1.62 **1.06**	0.01 **0.01**	13.9 **6.89**	NRT NRT	NRT NRT
8 9 10	Braking + cornering	70	100 m – 180°	ABS ESC R-ESC	75.86* 67.06 **62.61**	65.6 4.76 **2.93**	0.17 **0.01** 0.02	N/A N/A N/A	NRT NRT NRT	NRT NRT NRT
11 12	Fishhook	45	NA	ESC R-ESC	N/A N/A	23.50 **6.21**	0.12 **0.06**	**4.72** 7.49	10.36 **2.09**	0.49 **0.29**

Abbreviations: MATE – Mean Absolute Tracking Error; N/A - Not Applicable; NRT - No Rollover Threat observed
* Larger braking distance as brakes were actuated later.

1) Cornering-only evaluation: The objectives in the cornering-only tests are to ensure reference yaw tracking, minimise deviation from the lane, and minimise decrease in vehicle speed due to differential braking intervention. The open-loop test case demonstrates the vehicle undergoing the J-turn without any intervention for yaw correction. The truck departed from the lane, highlighting the need for intervention. The R-ESC ensured completion of the J-turn in contrast to the ESC, which was inherently designed for combined cornering plus braking, and hence due to excessive differential braking, it overcorrected and drifted off road. The yaw correction was much smoother in the R-ESC, which was designed to achieve this objective, unlike the ESC, which demonstrated excessive chattering as depicted in the Fig. 4. The decrease in velocity was also observed to be much less compared to the ESC formulation as presented in Tab. I.

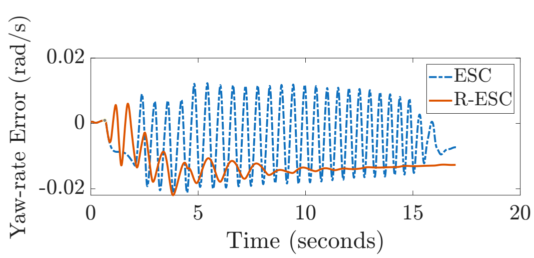

Fig. 4: Yaw-rate error during high-speed cornering maneuver.

2) Combined Cornering and emergency braking: In the case of combined cornering and braking (CCB) maneuvers, the vehicle follows the same cornering maneuver except for the driver demanding full braking 30 m into the curve to mimic a late reaction to an obstacle in the turn. Here, in addition to minimum yaw rate tracking error and lane deviation, the control unit is expected to help mitigate wheel lock and minimising stopping distance. The impact of the integrated framework is compared against open-loop and ABS without any ESC. As shown in Fig. 5, the R-ESC and ESC-intervened responses exhibit significantly lower yaw-rate error, resulting in improved lane tracking compared to the ABS-only response. It was noted that without ESC or R-ESC intervention, the vehicle suffered lane departure, although wheel lock was avoided in the ABS-intervened cases, as depicted in Fig. 6, due to exclusive use of available friction for longitudinal force rather than lateral force generation required for cornering. Since the cornering maneuver starts before the brake demand, both the ESC and R-ESC intervene by applying corrective brake pressure before the explicit brake demand by the driver, hence explaining the shorter stopping distances than the ABS-only mode. The ABS-only and ESC+ABS strategies resulted in more air consumption due to aggressive brake pressure modulation, whereas the R-ESC+ABS reduced air usage by nearly 20% through smoother corrective braking. While ESC achieved marginally better yaw-rate tracking, the R-ESC limited the peak sideslip more effectively owing to reduced chattering from the smoother tanh-based control formulation.

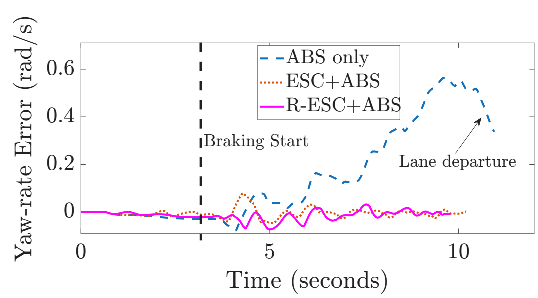

Fig. 5: Yaw-rate error during high-speed CCB maneuver.

3) Fishhook test: To test the untripped rollover propensity with algorithm intervention, fishhook maneuver is deployed. It was observed that without any intervention, the vehicle rolled over. The ESC-based formulation did not lead to a rollover, however, it was less effective in mitigating the risk as the LTR value remained at -1 for a prolonged

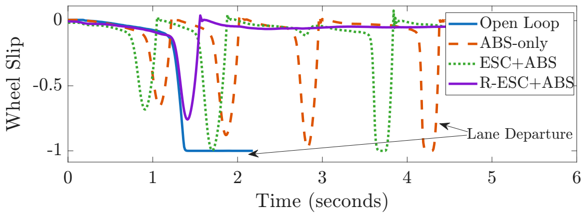

Fig. 6: Longitudinal wheel slip of the rear inner wheel during combined cornering and braking test.

Algorithm	ABS-Only	ESC+ABS	R-ESC+ABS
Yaw-rate tracking	↓↓	↑↑	↑
Cornering Speed drop	NA	↑	↓
Braking performance	↑↑	↑	↑
Roll Stability	↓	–	↑↑
Air consumption	↑	↑	–
Complexity	↓↓	↑↑	–

Fig. 8: Trade-offs and Impact of the proposed R-ESC.

period of time, which was mitigated by the proposed R-ESC formulation as depicted in Fig. 7.

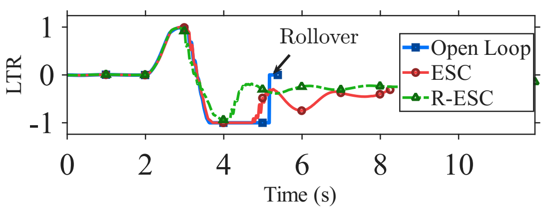

Fig. 7: LTR indicating rollover propensity.

IV. Conclusions

This study presented a roll-aware ESC framework tailored to HCRVs equipped with pneumatic brake systems, designed to perform adaptively across cornering-only and cornering plus full braking, including operation during ABS intervention. The proposed ESC was designed to mitigate roll and yaw instability using physics-motivated logical decisions. The HiL evaluation of the framework under cornering-only test showed superior performance with the proposed formulation allowing 38% speed drop as opposed to the 78% drop in the previous formulation during high-speed tests. Embedding roll-aware dynamics and lateral-load-transfer constraints using a physics motivated logic based framework enabled the proposed algorithm to outperform its predecessor in an excess roll manuever with minimal wheel lift-off time. The overall impact and trade-offs of the proposed ESC algorithm is depicted in Fig. 8. Despite these advantages, the proposed logic-based controller relies on calibration-sensitive parameters whose optimal selection may vary with vehicle and road friction conditions. The selected pressure distribution strategy and rollover thresholds selected for simplicity and practical implementation may not be globally optimal for all operating conditions. Therefore, the future work focuses on improving the robustness of the proposed algorithm, conducting a sensitivity analysis of the tuning parameters, and on-vehicle deployment.

References

[1] Ministry of Road Transport and Highways, "Road accidents in india 2023," https://morth.nic.in/backend/documents/uploaded/Road-Accident-in-India-2023-Publications.pdf, 2024, accessed: Mar. 4, 2026.

[2] H. B. Pacejka, *Tire and Vehicle Dynamics*, 3rd ed. Oxford, U.K.: Butterworth-Heinemann, 2012.

[3] National Highway Traffic Safety Administration, "Federal motor vehicle safety standards; electronic stability control systems for heavy vehicles," Federal Register, Jun. 2015, final rule establishing Federal Motor Vehicle Safety Standard No. 136.

[4] M. Ataei, A. Khajepour, and S. Jeon, "Model predictive control for integrated lateral stability, traction/braking control, and rollover prevention of electric vehicles," *Vehicle System Dynamics*, vol. 58, no. 1, pp. 49–73, 2020.

[5] M. D. Bernardis *et al.*, "On nonlinear model predictive direct yaw moment control with hitch angle measurement," *Vehicle System Dynamics*, vol. 61, no. 3, pp. 445–473, 2023.

[6] G. Tavolo, P. Stano, D. Tavernini, U. Montanaro, M. Tufo, G. Fiengo, P. Perlo, and A. Sorniotti, "Nonlinear model predictive control for enhanced path tracking and autonomous drifting through direct yaw moment control and rear-wheel-steering," in *Proceedings of the 16th International Symposium on Advanced Vehicle Control (AVEC)*, ser. Lecture Notes in Mechanical Engineering, Milan, Italy, 2024, pp. 854–861.

[7] F. Wang, X. Liu, G. Yin, L. Xu, J. Liang, and Y. Lu, "T-s fuzzy based model predictive control method for the direct yaw moment control system design," *Chinese Journal of Mechanical Engineering*, vol. 38, p. 150, 2025.

[8] H. Patil, K. B. Devika, and S. C. Subramanian, "Direct yaw-moment control integrated with wheel slip regulation for heavy commercial road vehicles," *IEEE Access*, vol. 10, pp. 116 284–116 300, 2022.

[9] C. C. MacAdam, "A computer-based study of the yaw/roll stability of heavy trucks characterized by high centers of gravity," in *SAE International Truck and Bus Meeting and Exposition*, 1982.

[10] B. Hopkins, S. Taheri, M. Ahmadian, and A. Reid, "Yaw stability control and emergency roll control for vehicle rollover mitigation," in *SAE 2010 Commercial Vehicle Engineering Congress*. SAE International, Oct. 2010.

[11] ZF Friedrichshafen AG, "Esc smart factsheet," https://www.zf.com/public/org/ESCsmartFactsheet_72320.pdf, accessed: Mar. 4, 2026.

[12] Knorr-Bremse AG, "Driver assistance systems – supporting drivers, maximizing traffic safety," https://truck.knorr-bremse.com/en/de/products/driver-assistance-systems/, accessed: Mar. 4, 2026.

[13] J. Velagic, "Design of smith-like predictive controller with communication delay adaptation," *World Academy of Science, Engineering and Technology*, vol. 47, pp. 199–203, 2008.

[14] P. V. Gaurkar, A. Challa, K. Ramakrushnan, G. Vivekanandan, S. Sivaram, and S. C. Subramanian, "Impact of effective tire radius on wheel slip estimation and antilock brake system performance of heavy road vehicles," *IEEE Transactions on Vehicular Technology*, vol. 71, no. 12, pp. 12 722–12 733, 2022.

[15] S. S. Devadiga, P. V. Gaurkar, G. Vivekanandan, S. Sivaram, and S. C. Subramanian, "A computationally and data-efficient reference slip estimation algorithm for antilock brake system," in *2023 9th International Conference on Control, Decision and Information Technologies (CoDIT)*, 2023, pp. 471–476.

[16] A. Challa, K. Ramakrushnan, P. V. Gaurkar, S. C. Subramanian, G. Vivekanandan, and S. Sivaram, "A 3-phase combined wheel slip and acceleration threshold algorithm for anti-lock braking in heavy commercial road vehicles," *Vehicle System Dynamics*, vol. 60, no. 7, pp. 2312–2333, 2022.

[17] Y. Cai *et al.*, "Hybrid physics and neural network model for lateral vehicle dynamics," *Proceedings of the Institution of Mechanical Engineers, Part D: Journal of Automobile Engineering*, 2024.

[18] D. Chu, Z. Li, J. Wang, C. Wu, and Z. Hu, "Rollover speed prediction on curves for heavy vehicles using mobile smartphone," *Measurement*, vol. 130, pp. 404–411, 2018.